



Journal of Mechanics of Materials and Structures

**THE EFFECT OF VARIABLE THERMAL CONDUCTIVITY
ON AN INFINITE FIBER-REINFORCED THICK PLATE
UNDER INITIAL STRESS**

Mohamed I. A. Othman, Ahmed E. Abouelregal and Samia M. Said

Volume 14, No. 2

March 2019



THE EFFECT OF VARIABLE THERMAL CONDUCTIVITY ON AN INFINITE FIBER-REINFORCED THICK PLATE UNDER INITIAL STRESS

MOHAMED I. A. OTHMAN, AHMED E. ABOUELREGAL AND SAMIA M. SAID

The present paper includes an analytical study of the effect of variable thermal conductivity and initial stress on a fiber-reinforced transversely isotropic thick plate. The model of the equations of generalized thermoelasticity with phase lags in an isotropic elastic medium with temperature-dependent mechanical properties are established. The upper surface of the plate is thermally insulated with prescribed surface loading while the lower surface of the plate rests on a rigid foundation and temperature. The normal mode analysis is used to obtain the analytical expressions of the displacement components, force stress and temperature distribution. Numerical results for the physical quantities are given and illustrated graphically with temperature-dependent and temperature-independent thermal conductivity. A comparison is made with results obtained with initial stress and without initial stress. Also, a comparison is made with results obtained with reinforcement and without reinforcement properties. It is found from the graphs that the initial stress, the reinforcement and phase lags have great effects on the distribution of the field quantities.

1. Introduction

Fiber-reinforced composites are used in a variety of structures due to their low weight and high strength. The analysis of stress and deformation of fiber-reinforced composite materials has been an important subject of solid mechanics for last three decades. The mechanical behavior of many fiber-reinforced composite materials is adequately modeled by the theory of linear elasticity for transversely isotropic materials, with the preferred direction coinciding with the fiber direction. In such composites the fibers are usually arranged in parallel straight lines. Other configurations are used. An example is that of circumferential reinforcement, for which the fibers are arranged in concentric circles, giving strength and stiffness in the tangential (or hoop) direction. The analysis of stress and deformation of fiber-reinforced composite materials has been an important subject of solid mechanics for last three decades. The characteristic property of a reinforced concrete member is that its components, namely concrete and steel, act together as a single anisotropic unit as long as they remain in the elastic condition, i.e., the two components are bound together so that there can be no relative displacement between them.

In the past few years, attention had been given to the problems of the generation and propagation of elastic waves in anisotropic elastic solid or layers of different configurations. The propagation of elastic waves in anisotropic media is fundamentally different from their propagation in isotropic media. The information obtained from such studies is important to seismologists and geophysicists to find the

Keywords: dual-phase-lag model, fiber-reinforced, initial stress, normal mode analysis, variable thermal conductivity, thick plate.

location of the earthquakes as well as their energy, mechanism etc. and thereby gives valuable insight into the global tectonics. Some hard and soft rocks beneath the earth's surface show the reinforcement properties, i.e., the different components act as a single anisotropic unit. These rocks when come in the way of seismic waves do affect their propagation and such seismic signals are always influenced by the elastic properties of the media through which they travel. Fiber-reinforced composites are used in a variety of structures due to their low weight and high strength. A continuum model is used to explain the mechanical properties of such materials. In the case of an elastic solid reinforced by a series of parallel fibers, it is usual to assume transverse isotropy.

In the linear case, the associated constitutive relations, relating infinitesimal stress and strain components, have five materials constants. The idea of introducing a continuous self reinforcement at every point of an elastic solid was given by Belfield et al. [1983]. The model was later applied to the rotation of a tube by Verma and Rana [1983]. Sengupta and Nath [2001] discussed the problem of the surface waves in fiber-reinforced anisotropic elastic media. Hashin and Rosen [1964] gave the elastic moduli for fiber-reinforced materials. The two-dimensional problems of the generalized magneto-thermoelasticity in a fiber-reinforced anisotropic half-space was discussed by Abbas et al. [2011]. Othman and Abbas [2011] discussed the effect of rotation on plane waves at the free surface of a fiber-reinforced thermoelastic half-space using the finite element method. Ailawalia and Budhiraja [2011] discussed the effect of hydrostatic initial stress on fiber-reinforced generalized thermoelastic medium. Abbas and Abd-alla [2011] studied the effect of initial stress on a fiber-reinforced anisotropic thermoelastic thick plate. Othman and Said [2012] investigated the effect of rotation on the two-dimensional problem of a fiber-reinforced thermoelastic with one relaxation time.

The theory of thermoelasticity including the effect of temperature change has been well established. According to this theory, the temperature field is coupled with the elastic strain field. In thermoelasticity, classical heat transfer, Fourier's conduction equation is extensively used in many engineering applications. The classical theory of thermoelasticity by Nowacki [1975; 1986] rests upon the hypothesis of the Fourier law of heat conduction, in which the temperature distribution is governed by a parabolic-type partial differential equation. Consequently, the theory predicts that a thermal signal is felt instantaneously everywhere in a body. This implies that an infinite speed of propagation of the thermal signal, which is impractical from the physical point of view, particularly for short-time. Thus, the use of Fourier's equation may result in discrepancies under some special conditions, such as low-temperature heat transfer, high frequency or ultrahigh heat flux heat transfer.

The theory of the classical uncoupled theory of thermoelasticity predicts two phenomena not compatible with physical observations. First, the equation of heat conduction of this theory does not contain any elastic term contrary to the fact that the elastic changes produce heat effects. Second, the heat equation is of parabolic type predicting infinite speeds of propagation for heat waves. Biot [1956] introduced the theory of coupled thermoelasticity to overcome the first shortcoming.

Generalized thermoelasticity theories have been developed with the objective of removing the paradox of infinite speed of heat propagation inherent in the conventional coupled dynamical theory of thermoelasticity in which the parabolic type heat conduction equation is based on Fourier's law of heat conduction.

Lord and Shulman [1967] introduced a theory of generalized thermoelasticity with one relaxation time for an isotropic body. In this theory, a modified law of heat conduction, including both the heat flux and its time derivatives replaces the conventional Fourier's law. The heat equation associated with this theory

is hyperbolic and hence eliminates the paradox of infinite speeds of propagation inherent in both coupled and uncoupled theories of thermoelasticity. Green and Lindsay [1972] extended the coupled theory of thermoelasticity by introducing the thermal relaxation times in the constitutive equations. The theory of thermoelasticity without energy dissipation is another generalized theory and was formulated by Green and Naghdi [1993]. It includes the “thermal displacement gradient” among its independent constitutive variables, and differs from the previous theories in that it does not accommodate dissipation of thermal energy. Tzou [1996; 1995a] proposed the dual-phase-lag DPL model, which describes the interaction between phonons and electrons on the microscopic level as retarding sources causing a delayed response on the macroscopic scale. For macroscopic formulation, it would be convenient to use the DPL model for investigation of the micro-structural effect on the behavior of heat transfer. The DPL proposed by Chandrasekharaiah [1986] and Tzou [1995b] is such a modification of the classical thermoelastic model in which the Fourier law is replaced by an approximation to a modified Fourier law with two different time translations: a phase lag of the heat flux τ_q and a phase lag of temperature gradient τ_θ . A Taylor series approximation of the modified Fourier law, together with the remaining field equations leads to a complete system of equations describing a DPL thermoelastic model. The model transmits thermoelastic disturbance in a wavelike manner if the approximation is linear with respect to τ_q and τ_θ , and $0 \leq \tau_\theta < \tau_q$; or quadratic in τ_q and linear in τ_θ , with $\tau_q > 0$ and $\tau_\theta > 0$. This theory is developed in a rational way to produce a fully consistent theory which is able to incorporate thermal pulse transmission in a very logical manner. It includes the “thermal displacement gradient” among its independent constitutive variables, and differs from the previous theories in that it does not accommodate dissipation of thermal energy [Ignaczak and Ostoja-Starzewski 2010]. Said and Othman [2017] studied the effect of mechanical force, rotation and moving internal heat source on a two-temperature fiber-reinforced thermoelastic medium with two theories. Abouelregal [2011] applied the DPL heat transfer model for an isotropic solid sphere.

The solution of the problem is carried out when the boundary of the sphere is maintained at constant heat flux and the displacement of the surface is constrained. Abdallah [2009] used the uncoupled thermoelastic model based on the DPL heat conduction equation to investigate the thermoelastic properties of a semi-infinite medium induced by a homogeneously illuminating ultrashort pulsed laser heating. Quintanilla and Jordan [2009] present exact solutions of two initial-boundary value problems in the setting of a recently introduced theory of heat conduction, wherein the two temperature theory of the late 1960s is merged with Tzou’s DPL flux relation.

The development of initial stresses in the medium is due to many reasons, for example, resulting from differences of temperature, process of quenching, shot pinning and cold working, slow process of creep, differential external forces, gravity variations, etc. The earth is assumed to be under high initial stresses. It is, therefore, of much interest to study the influence of these stresses on the propagation of stress waves. Biot [1965] showed the acoustic propagation under initial stress, which is fundamentally different from that under a stress-free state. He has obtained the velocities of longitudinal and transverse waves along the coordinate axis only.

The wave propagation in solids under initial stresses has been studied by many authors for various models. The study of the effects of gravitational and hydrostatic initial stress on a two-temperature fiber-reinforced thermoelastic medium for three-phase-lag is due to Said and Othman [2016], Montanaro [1999] investigated the isotropic linear thermoelasticity with hydrostatic initial stress. Abbas and Othman [2012], Othman et al. [2013] and Sarkar et al. [2016] studied the effect of the hydrostatic initial stress, the

gravity and the magnetic field on a fiber-reinforced thermoelastic medium with a fractional derivative heat transfer. Ailawalia et al. [2009] investigated deformation in a generalized thermoelastic medium with hydrostatic initial stress.

In this study, the dual phase lag theory is applied to study the two-dimensional problem of generalized thermoelasticity for a fiber-reinforced thick plate under initial stress and variable thermal conductivity. The problem is solved numerically using a normal mode analysis method. Numerical results for the temperature distribution and the displacement and stress components are given and illustrated graphically. It is found from the graphs that variability thermal conductivity parameter and the initial stress significantly influences the variations of field quantities. This article is a continuation of the work by Abbas and Abd-alla [2011] and Othman and Said [2012] to include the effect of reference temperature on thermal stress distribution.

2. Basic equations

The linear equations governing thermoelastic interactions in a homogeneous transversely isotropic fiber-reinforced solid without any heat sources or body forces with hydrostatic initial stress in the context of generalized thermoelasticity with dual phase lags are given now.

The equation of motion in the absence of body forces can be written as

$$\sigma_{ij,j} + (u_{i,k} \sigma_{kj}^0)_{,j} = \rho \frac{\partial^2 u_i}{\partial t^2}, \quad (1)$$

where σ_{ij} are the components of stress, σ_{kj}^0 is the initial stress tensor, ρ is the density, u_i are the components of displacement vector and $i, j, k = 1, 2, 3$. The comma denotes space-coordinate differentiation and the repeated index in the subscript implies summation.

The heat conduction equation corresponding to the DPL model proposed by Tzou [1996] takes the form

$$\left(1 + \tau_\theta \frac{\partial}{\partial t}\right) (K_{ij} \theta_{,j})_{,i} = \left(\delta + \tau_q \frac{\partial}{\partial t}\right) \left(\rho C_E \frac{\partial T}{\partial t} + \beta_{ij} T_0 u_{i,j}\right), \quad (2)$$

where K_{ij} is the thermal conductivity, C_E is the specific heat at constant strain, $\theta = T - T_0$ is the temperature increment of the resonator, in which T_0 is the environmental temperature, assumed to be such as $|(T - T_0)/T| \ll 1$, β_{ij} is the thermal elastic coupling tensor, τ_q is the phase lag of the heat flux, τ_θ is the phase lag of the gradient of temperature where $0 \leq \tau_\theta < \tau_q$.

The constitutive equations for a fiber-reinforced linearly elastic anisotropic medium with respect to the reinforcement direction $\mathbf{b} \equiv (b_1, b_2, b_3)$, with $b_1^2 + b_2^2 + b_3^2 = 1$ are

$$\begin{aligned} \sigma_{ij} = & \lambda e_{kk} \delta_{ij} + 2\mu_T e_{ij} + \alpha (b_k b_m e_{km} \delta_{ij} + b_i b_j e_{kk}) + 2(\mu_L - \mu_T) (b_k b_i e_{kj} + b_k b_j e_{ki}) \\ & + \beta b_k b_m e_{km} b_i b_j - \beta_{ij} (T - T_0), \end{aligned} \quad (3)$$

where e_{ij} are the components of strain, λ, μ_T are the elastic constants, $\alpha, \beta, \mu_L - \mu_T$ are the reinforcement parameters, and δ_{ij} is Kronecker's delta.

Strain-displacement relations

$$e_{ij} = \frac{1}{2} (u_{i,j} + u_{j,i}). \quad (4)$$

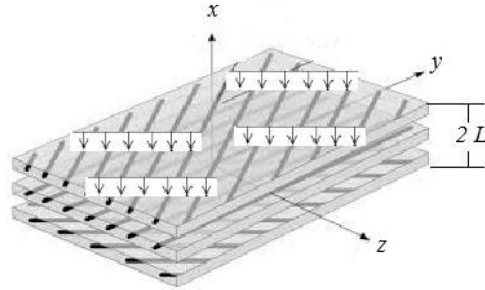


Figure 1. Geometry of the problem.

In physics, thermal conductivity is the property of a material’s ability to conduct heat. It appears primarily in Fourier’s law for heat conduction. Thermal conductivity is measured in watt per Kelvin per meter ($\text{W K}^{-1} \text{m}^{-1}$) multiplied by a temperature difference and an area, and divided by a thickness, the thermal conductivity predicts the rate of energy loss through a piece of material. In the window building industry “thermal conductivity” is expressed as the U-Factor, which measures the rate of heat transfer and tells you how well the window insulates.

3. Formulation of the problem

In the present paper, we consider an infinite thick plate with traction free surfaces at $x = \pm L$ (layer of thickness $2L$), which consists of homogeneous, transversely isotropic thermoelastic material. We take the origin of the coordinate system (x, y, z) on the middle surface of the layer. The $x - y$ plane is chosen to coincide with the middle surface and y axis normal to it along the thickness. Then the components of the displacement vector and temperature are independent of z and can be taken in the following forms

$$u = u(x, y, t), \quad v = v(x, y, t), \quad w = 0, \quad \theta = \theta(x, y, t). \tag{5}$$

The constitutive relations and field equations with an initial stress and without body forces and heat sources in the present case are

$$\sigma_{xx} = (\lambda + 2\alpha + 4\mu_L - 2\mu_T + \beta) \frac{\partial u}{\partial x} + (\lambda + \alpha) \frac{\partial v}{\partial y} - \beta_{11}(T - T_0), \tag{6}$$

$$\sigma_{yy} = (\lambda + 2\mu_T) \frac{\partial v}{\partial y} + (\lambda + \alpha) \frac{\partial u}{\partial x} - \beta_{22}(T - T_0), \tag{7}$$

$$\sigma_{xy} = \mu_L \left(\frac{\partial v}{\partial x} + \frac{\partial u}{\partial y} \right), \tag{8}$$

where \mathbf{b} is chosen so that its components are $(1, 0, 0)$.

The equations of motion along x and y directions can be obtained as

$$[\lambda + 2(\alpha + \mu_T) + 4(\mu_L - \mu_T) + \beta + \sigma_0] \frac{\partial^2 u}{\partial x^2} + (\sigma_0 + \mu_L) \frac{\partial^2 u}{\partial y^2} + (\alpha + \lambda + \mu_L) \frac{\partial^2 v}{\partial x \partial y} - \beta_{11} \frac{\partial T}{\partial x} = \rho \frac{\partial^2 u}{\partial t^2}, \tag{9}$$

$$(\lambda + 2\mu_T + \sigma_0) \frac{\partial^2 v}{\partial y^2} + (\sigma_0 + \mu_L) \frac{\partial^2 v}{\partial x^2} + (\alpha + \lambda + \mu_L) \frac{\partial^2 u}{\partial x \partial y} - \beta_{22} \frac{\partial T}{\partial y} = \rho \frac{\partial^2 v}{\partial t^2}, \tag{10}$$

where σ_0 is the initial pressure and

$$\beta_{11} = (2\lambda + 3\alpha + 4\mu_L - 2\mu_T + \beta)\alpha_{11} + (\lambda + \alpha)\alpha_{22}, \quad \beta_{22} = (2\lambda + \alpha)\alpha_{11} + (\lambda + 2\mu_T)\alpha_{22}. \quad (11)$$

The heat equation can be written as

$$\left(1 + \tau_\theta \frac{\partial}{\partial t}\right) \left[\frac{\partial}{\partial x} \left(K_{11} \frac{\partial \theta}{\partial x} \right) + \frac{\partial}{\partial y} \left(K_{22} \frac{\partial \theta}{\partial y} \right) \right] = \left(\delta + \tau_q \frac{\partial}{\partial t} \right) \left[\rho C_E \frac{\partial \theta}{\partial t} + T_0 \frac{\partial}{\partial t} \left(\beta_{11} \frac{\partial u}{\partial x} + \beta_{22} \frac{\partial v}{\partial y} \right) \right]. \quad (12)$$

Modern structural elements are often subjected to temperature changes of such magnitude that their material properties may no longer be regarded as having constant values even in an approximate sense. The thermal and mechanical properties of materials vary with temperature, so that the temperature dependence of material properties must be taken into consideration in the thermal stress analysis of these elements. In physics, thermal conductivity is the property of a material to conduct heat. It is evaluated primarily in terms of Fourier's law for heat conduction. Heat transfer occurs at a higher rate across materials of higher thermal conductivity than across materials of low thermal conductivity. Generally, thermal conductivity of materials is temperature dependent.

Our goal is to investigate the effect of temperature dependency of thermal conductivity keeping the other elastic and thermal parameter constants; therefore we assume the thermal conductivities and thermal diffusivity are assumed to vary linearly with temperature according to

$$K_{11} = K_{11}(\theta) = K_{01}(1 + K_1\theta), \quad K_{22} = K_{22}(\theta) = K_{02}(1 + K_1\theta), \quad \rho C_E = \rho C_E(\theta) = \rho_0 C_{E0}(1 + K_1\theta), \quad (13)$$

where K_{01} , K_{02} , ρ_0 and C_{E0} are considered constants, in case of temperature-independent modulus of elasticity $K_1 = 0$.

Now, using the mapping [Tzou 1996]:

$$\psi = \int_0^\theta (1 + K_1\xi) d\xi, \quad (14)$$

where ψ is a new function expressing the heat conduction.

From (14), we get

$$\psi = \theta \left(1 + \frac{1}{2} K_1 \theta \right). \quad (15)$$

Differentiating (15) with respect to x and y , we obtain

$$K_{01} \frac{\partial \psi}{\partial x} = K_{11}(\theta) \frac{\partial \theta}{\partial x}, \quad K_{02} \frac{\partial \psi}{\partial y} = K_{22}(\theta) \frac{\partial \theta}{\partial y}. \quad (16)$$

With the same manner, by differentiating the mapping with respect to time t , we have

$$\rho_0 C_{E0} \frac{\partial \psi}{\partial t} = \rho C_E \frac{\partial \theta}{\partial t}. \quad (17)$$

Using (16) and (17), the modified model of heat equation will take the form

$$\left(1 + \tau_q \frac{\partial}{\partial t} \right) \left[\rho_0 C_{E0} \frac{\partial \psi}{\partial t} + T_0 \frac{\partial}{\partial t} \left(\beta_{11} \frac{\partial u}{\partial x} + \beta_{22} \frac{\partial v}{\partial y} \right) \right] = \left(1 + \tau_\theta \frac{\partial}{\partial t} \right) \left[K_{01} \frac{\partial^2 \psi}{\partial x^2} + K_{02} \frac{\partial^2 \psi}{\partial y^2} \right]. \quad (18)$$

For simplification, we shall use the following nondimensional variables:

$$\begin{aligned} x' &= c_0 \eta x, & y' &= c_0 \eta y, & u' &= c_0 \eta u, & v' &= c_0 \eta v, & t' &= c_0^2 \eta t, \\ \sigma'_0 &= \frac{\sigma_0}{\rho_0 c_0^2}, & \sigma'_{ij} &= \frac{\sigma_{ij}}{\rho_0 c_0^2}, & \tau'_q &= c_0^2 \eta \tau_q, & \tau'_\theta &= c_0^2 \eta \tau_\theta, & \psi' &= \frac{\beta_{11} \psi}{\rho_0 c_0^2}. \end{aligned} \quad (19)$$

where,

$$c_0^2 = \frac{A_{11}}{\rho_0}, \quad A_{11} = \lambda + 2(\alpha + \mu_T) + 4(\mu_L - \mu_T) + \beta, \quad \eta = \frac{\rho_0 C_{E0}}{K_{01}}.$$

The thermal property variations are assumed to be small and the approximate symmetries of the equation are calculated. A linear functional variation is assumed for the thermal properties and a similarity solution is constructed. For linearity, such that $|\theta/T_0| \ll 1$, then equations of motion, with the help of (16), may be recast into the dimensionless form after suppressing the primes as

$$(1 + \sigma_0) \frac{\partial^2 u}{\partial x^2} + (\sigma_0 + B_4) \frac{\partial^2 u}{\partial y^2} + (B_1 + B_4) \frac{\partial^2 v}{\partial x \partial y} - \frac{\partial \psi}{\partial x} = \frac{\partial^2 u}{\partial t^2}, \quad (20)$$

$$(B_2 + \sigma_0) \frac{\partial^2 v}{\partial y^2} + (\sigma_0 + B_4) \frac{\partial^2 v}{\partial x^2} + (B_1 + B_4) \frac{\partial^2 u}{\partial x \partial y} - B_3 \frac{\partial \psi}{\partial y} = \frac{\partial^2 v}{\partial t^2}, \quad (21)$$

$$\left(1 + \tau_\theta \frac{\partial}{\partial t}\right) \left(\frac{\partial^2 \psi}{\partial x^2} + \varepsilon_1 \frac{\partial^2 \psi}{\partial y^2}\right) = \left(\delta + \tau_q \frac{\partial}{\partial t}\right) \left[\frac{\partial \psi}{\partial t} + \frac{\partial}{\partial t} \left(\varepsilon_2 \frac{\partial u}{\partial x} + \varepsilon_3 \frac{\partial v}{\partial y}\right)\right]. \quad (22)$$

The constitutive relations given in (1) in dimensionless forms and for linearity take the form

$$\sigma_{xx} = \frac{\partial u}{\partial x} + B_1 \frac{\partial v}{\partial y} - \psi, \quad (23)$$

$$\sigma_{xy} = B_4 \left(\frac{\partial u}{\partial y} + \frac{\partial v}{\partial x}\right), \quad (24)$$

where

$$\begin{aligned} B_1 &= \frac{A_{12}}{A_{11}}, & B_2 &= \frac{A_{22}}{A_{11}}, & B_3 &= \frac{\beta_{22}}{\beta_{11}}, & B_4 &= \frac{\mu_L}{A_{11}}, & A_{12} &= \alpha + \lambda, & A_{22} &= \lambda + 2\mu_T, \\ \varepsilon_1 &= \frac{K_{02}}{K_{01}}, & \varepsilon_2 &= \frac{\beta_{11}^2 T_0}{\rho_0 C_{E0} A_{11}}, & \varepsilon_3 &= \frac{\beta_{11} \beta_{22} T_0}{\rho_0 C_{E0} A_{11}}. \end{aligned}$$

4. Normal mode analysis

The normal mode analysis gives exact solutions without any assumed restrictions on the temperature, displacement, and stress distributions. It is applied to a wide range of problems in different branches. It can be applied to boundary-layer problems, which are described by the linearized Navier–Stokes equations in electro-hydro-dynamics. The normal mode analysis is, in fact, to look for the solution in the Fourier transformed domain, assuming that all the field quantities are sufficiently smooth on the real line so that the normal mode analysis of these functions exists. The normal mode expansion method has been proposed by Cheng et al. [2000] for modeling the thermoelastic generation process of elastic waveforms in an isotropic plate.

The solution of the considered physical variable can be decomposed in terms of normal modes as the following form

$$[u, v, \psi, \sigma_{ij}](x, y, t) = [u^*, v^*, \psi^*, \sigma_{ij}^*](x) e^{\omega t + i a y}, \quad (25)$$

where ω is the (complex) frequency constant, $i = \sqrt{-1}$, a is the wave number in the y direction, and $u^*(x)$, $v^*(x)$, $\psi^*(x)$ and $\sigma_{ij}^*(x)$ are the amplitudes of the field quantities.

Using (25), (20)–(24) take the forms

$$\left(\frac{d^2}{dx^2} - g_1\right)u^* + g_2 \frac{dv^*}{dx} = g_3 \frac{d\psi^*}{dx}, \quad (26)$$

$$\left(\frac{d^2}{dx^2} - g_4\right)v^* + g_5 \frac{du^*}{dx} = g_6 \psi^*, \quad (27)$$

$$\left(\frac{d^2}{dx^2} - g_7\right)\psi^* = g_8 \frac{du^*}{dx} + g_9 v^*, \quad (28)$$

$$\sigma_{xx}^* = \frac{du^*}{dx} + iaB_1 v^* - \psi^*, \quad (29)$$

$$\sigma_{xy}^* = B_4 \left(iau^* + \frac{dv^*}{dx}\right), \quad (30)$$

where

$$g_1 = \frac{a^2(\sigma_0 + B_4)}{1 + \sigma_0} + \frac{\omega^2}{1 + \sigma_0}, \quad g_2 = \frac{ia(B_1 + B_4)}{1 + \sigma_0}, \quad g_3 = \frac{1}{1 + \sigma_0}, \quad g_4 = \frac{a^2(\sigma_0 + B_2) + \omega^2}{\sigma_0 + B_4},$$

$$g_5 = \frac{ia(B_1 + B_4)}{\sigma_0 + B_4}, \quad g_6 = \frac{iaB_3}{\sigma_0 + B_4}, \quad g_7 = a^2 \varepsilon_1 + \frac{\omega(\delta + \tau_q \omega)}{1 + \tau_\theta \omega}, \quad g_8 = \frac{\varepsilon_2 \omega(\delta + \tau_q \omega)}{1 + \tau_\theta \omega}, \quad g_9 = \frac{ia \varepsilon_3 \omega(\delta + \tau_q \omega)}{1 + \tau_\theta \omega}.$$

Eliminating $\psi^*(x)$ and $v^*(x)$ in (26)–(28), one obtains

$$(D^6 - AD^4 + BD^2 - C)u^*(x) = 0, \quad (31)$$

where

$$D = \frac{d}{dx}, \quad A = g_3 g_8 + g_2 g_5 + g_1 + g_4 + g_7,$$

$$B = g_2 g_5 g_7 + g_2 g_6 g_8 + g_3 g_4 g_8 + g_1 g_4 + g_1 g_7 + g_4 g_7 - g_6 g_9 + g_3 g_5 g_9, \quad C = g_1 g_4 g_7 - g_1 g_6 g_9.$$

Equation (31) can be factorized as

$$(D^2 - k_1^2)(D^2 - k_2^2)(D^2 - k_3^2)u^*(x) = 0, \quad (32)$$

where k_n^2 ($n = 1, 2, 3$) are the roots of the following characteristic equation:

$$k^6 - Ak^4 + Bk^2 - C = 0. \quad (33)$$

The solution of (31), bound at $x \rightarrow \infty$, is given by

$$u^*(x) = \sum_{n=1}^3 M_{1n} e^{-k_n x}. \quad (34)$$

In a similar manner, one gets

$$\psi^*(x) = \sum_{n=1}^3 H_{1n} M_{1n} e^{-k_n x}, \quad v^*(x) = \sum_{n=1}^3 H_{2n} M_{1n} e^{-k_n x}, \quad (35)$$

where

$$H_{1n} = \frac{(g_5 g_9 + g_4 g_8)k_n - g_8 k_n^3}{k_n^4 - (g_4 + g_7)k_n^2 + (g_4 g_7 - g_6 g_9)}, \quad H_{2n} = \frac{g_8 k_n + (k_n^2 - g_7)H_{1n}}{g_9}.$$

Introducing (34)–(35) into (29) and (30), we obtain

$$\sigma_{xx}^* = \sum_{n=1}^3 H_{3n} M_{1n} e^{-k_n x}, \quad \sigma_{xy}^* = \sum_{n=1}^3 H_{4n} M_{1n} e^{-k_n x}, \quad (36)$$

where $H_{3n} = -k_n + iaB_1 H_{2n} - H_{1n}$, $H_{4n} = B_4(ia - k_n H_{3n})$.

5. Boundary conditions

In this section we determine the parameters M_{1n} ($n = 1, 2, 3$). In the physical problem, we should suppress the positive exponentials that are unbounded at infinity. The constants M_{11} , M_{12} , M_{13} have to be chosen such that the boundary conditions on the surface at $x = L$ take the form

$$\sigma_{xx}(L, y, t) = -P_1 f, \quad \sigma_{xy}(L, y, t) = 0, \quad \psi(L, y, t) = P_3, \quad (37)$$

where f is constant, P_1 is the magnitude of a hydrostatic initial stress and $P_3 = P_2 + \frac{1}{2}K_1 P_2^2$. If $P_2 = 0$, we obtain the corresponding expressions for normal force applied on the plane surface. If we put $P_1 = 0$, then the corresponding expressions yield the results for thermal sources.

Substituting the expressions of the variables considered into the above boundary conditions, we obtain

$$\psi^*|_{x=L} = \sum_{n=1}^3 H_{1n} M_{1n} e^{-k_n x} = P_3^*, \quad (38)$$

$$\sigma_{xx}^*|_{x=L} = \sum_{n=1}^3 H_{3n} M_{1n} e^{-k_n x} = -P_1^*, \quad (39)$$

$$\sigma_{xy}^*|_{x=L} = \sum_{n=1}^3 H_{4n} M_{1n} e^{-k_n x} = 0, \quad (40)$$

where $P_1^* = P_1 e^{-(\omega t + iay)}$, $P_3^* = P_3 e^{-(\omega t + iay)}$.

Solving the above system of (38)–(40), we obtain a system of three equations. After applying the inverse of the matrix method, we have the values of the three constants M_{1n} ($n = 1, 2, 3$). Hence, we obtain the expressions for the displacements, the temperature distribution, and other physical quantities:

$$\begin{pmatrix} M_{11} \\ M_{12} \\ M_{13} \end{pmatrix} = \begin{pmatrix} H_{11} e^{-k_1 L} & H_{12} e^{-k_2 L} & H_{13} e^{-k_3 L} \\ H_{31} e^{-k_1 L} & H_{32} e^{-k_2 L} & H_{33} e^{-k_3 L} \\ H_{41} e^{-k_1 L} & H_{42} e^{-k_2 L} & H_{43} e^{-k_3 L} \end{pmatrix}^{-1} \begin{pmatrix} P_3^* \\ -P_1^* \\ 0 \end{pmatrix}. \quad (41)$$

After obtaining ψ , the temperature increment θ can be obtained by solving (15) to give

$$\theta = \frac{-1 + \sqrt{1 + 2K_1 \psi}}{K_1}. \quad (42)$$

6. Particular cases

- (1) Generalized thermoelastic medium with hydrostatic initial stress and with temperature-dependent thermal conductivity from above equations with $\mu_L = \mu_T = \mu$, $\alpha = \beta = 0$.
- (2) Fiber-reinforced generalized thermoelastic medium without hydrostatic initial stress and with temperature-dependent thermal conductivity from above equations with $P_1 = \sigma_0 = 0$.
- (3) Fiber-reinforced generalized thermoelastic medium without temperature-dependent thermal conductivity from above equations with $K_1 = 0$.
- (4) Equation of coupled thermoelasticity (CD theory) when $\tau_\theta = \tau_q = 0$, $\delta = 1$.
- (5) Lord–Shulman theory (LS theory) $\tau_\theta = 0$, $\delta = 1$, $\tau_q > 0$.
- (6) Green–Naghdi theory (GN II theory) when $\tau_\theta = 0$, $\delta = 0$, $\tau_q = 1$.
- (7) Equations of generalized thermoelasticity with phase lags (DPL theory) when $\delta = 1$, $\tau_q \geq \tau_\theta > 0$.

7. Numerical results

In order to illustrate the theoretical results obtained in the preceding section and to compare these in the context of the DPL model, the CD theory and the LS theory, we now present some numerical results for the physical constants as $\lambda = 3.76 \cdot 10^9 \text{ N/m}^2$, $\mu_T = 1.89 \cdot 10^{10} \text{ N/m}^2$, $\mu_L = 2.45 \cdot 10^{10} \text{ N/m}^2$, $\alpha = -1.28 \cdot 10^{10} \text{ N/m}^2$, $\beta = 0.32 \cdot \text{N/m}^2$, $\tau_q = 0.95 \text{ s}$, $C_{E0} = 23.1 \text{ J/(kg K)}$, $\rho_0 = 7800 \text{ kg/m}^3$, $\mu = 3.86 \cdot 10^{10} \text{ N/m}^2$, $\alpha_{11} = 1.7 \cdot 10^{-5} \text{ K}^{-1}$, $\alpha_{22} = 1.5 \cdot 10^{-5} \text{ K}^{-1}$, $\tau_\theta = 0.8 \text{ s}$, $K_{01} = 9.21 \cdot 10^5 \text{ J/(ms K)}$, $K_{02} = 9.63 \cdot 10^5 \text{ J/(ms K)}$, $\omega = \omega_0 + i\xi$, $\omega_0 = 0.6$, $\xi = 0.2$, $a = 0.5$, $P_1 = 30$, $L = 0.1 \text{ m}$, $T_0 = 293 \text{ K}$, $K_1 = -5$, $f = 1$, $P_2 = 0.5$, $\sigma_0 = 1.45 \cdot 10^8 \text{ N/m}^2$, $\alpha_t = 1.78 \cdot 10^{-5} \text{ K}^{-1}$, $P = 0.5$.

The computations were carried out for a value of time $t = 0.3$. The variations of the thermal temperature θ , the horizontal displacement u , and the stress components σ_{xx} , σ_{xy} with distance x for the value of y , namely $y = 1.5$, were substituted in performing the computation. The results are shown in Figures 2–12. The graphs show the six curves predicted by three different theories of thermoelasticity. In these figures, the solid line represents the solution in the coupled theory, the dotted line represents the solution in the generalized LS theory, and the dashed line represents the solution derived using the DPL model. Here all the variables are taken in nondimensional forms and the physical quantities depend not only on space x and time t , but also on phase lags τ_θ and τ_q .

Figures 2–5 show comparisons between the horizontal displacement components u , the thermal temperature θ and the stress components σ_{xx} , σ_{xy} with temperature-dependent and temperature-independent thermal conductivity. Figure 2 depicts that the distribution of the horizontal displacement u begins from positive values. In the context of the three theories, u starts with decreasing, then increases, and again decreases. The values of u , increasing with the temperature-dependent thermal conductivity in the first and then, decrease. It is clear from Figure 3 that the thermal temperature θ begins from negative values with temperature-dependent thermal conductivity, but it begins from positive values with temperature-independent thermal conductivity and satisfies the boundary condition at $x = 0.1$. In the context of the three theories with temperature-dependent thermal conductivity, θ increases in the range $0 \leq x \leq 6$, but with the temperature-independent thermal conductivity, θ decreases in the range $0 \leq x \leq 6$. The values

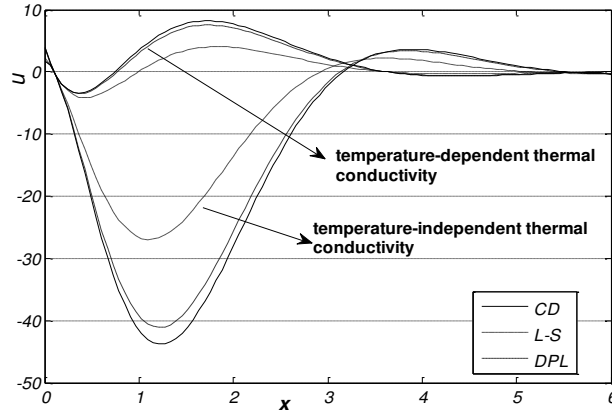


Figure 2. Horizontal displacement distribution u with temperature-dependent and temperature-independent thermal conductivity.

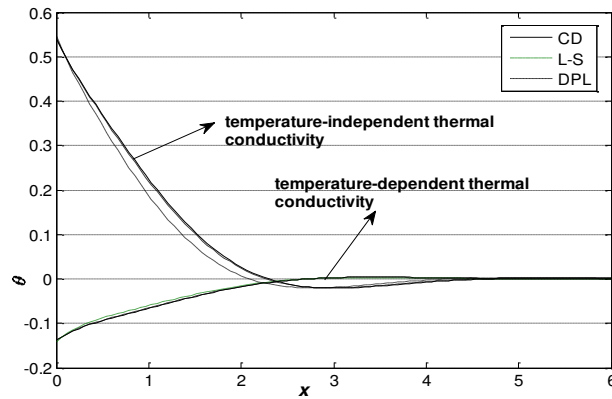


Figure 3. Thermal temperature distribution θ with temperature-dependent and temperature-independent thermal conductivity.

of θ decrease and then increasing with temperature-dependent thermal conductivity. Therefore, the effect of temperature-dependent thermal conductivity should be taken into consideration.

Figure 4 displays that the distribution of the stress component σ_{xx} begins from negative values and satisfies the boundary condition at $x = 0.1$. In the context of the three theories with temperature-dependent thermal conductivity, σ_{xx} starts with increasing, then decreases, and again increases. However, the context of the three theories with temperature-independent thermal conductivity, σ_{xx} starts with decreasing to a minimum value, then increases to a maximum value, and again decreases. The temperature-dependent thermal conductivity increase, then decrease, and last increase values of σ_{xx} . Figure 5 shows the distribution of the stress component σ_{xy} and demonstrates that it reaches a zero value and satisfies the boundary condition at $x = 0.1$. In the context of the three theories with temperature-dependent thermal conductivity, σ_{xy} starts with increasing, and then decreases.

However, in the context of the three theories with temperature-independent thermal conductivity, σ_{xy} starts with decreasing to a minimum value, then increase to a maximum value, and again decreases. The

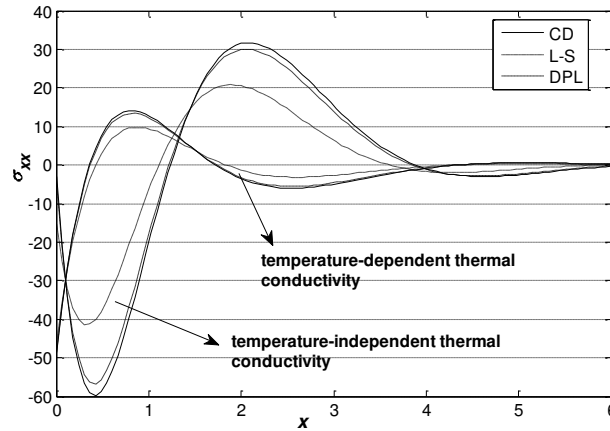


Figure 4. Distribution of stress component σ_{xx} with temperature-dependent and temperature-independent thermal conductivity.

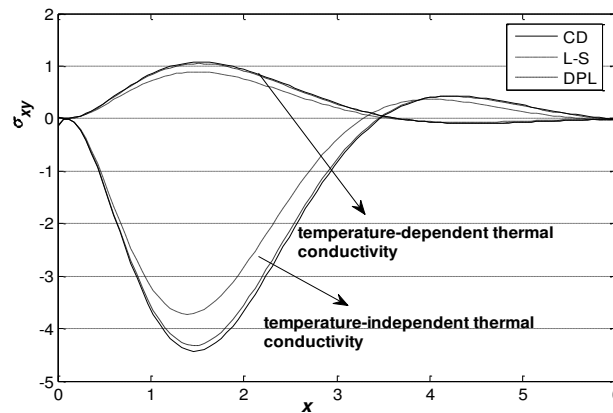


Figure 5. Distribution of stress component σ_{xy} with temperature-dependent and temperature-independent thermal conductivity.

values of σ_{xy} increase and then, decrease with temperature-dependent thermal conductivity. Figures 2–5 demonstrate that the temperature-dependent thermal conductivity has a significant role on all the physical quantities. The result provides a motivation to investigate the thermoelastic materials with temperature-dependent thermal conductivity as a new class of applications thermoelastic materials.

Also, the results obtained in this case should be useful for physicists, researchers in material science, designers of new materials as well as for those working on the development of thermal stresses and in practical situations as in optics, geophysics, geomagnetic, acoustics and oil prospecting.

Figures 6–9 show comparisons between the horizontal displacement components u , the thermal temperature θ , and the stress components σ_{xx} , σ_{xy} with and without the initial stress. Figure 6 depicts that the distribution of the horizontal displacement u begins from positive values. In the context of the three theories without initial stress, u decreases in the range $0 \leq x \leq 6$. The values of u increase with initial stress in the first and then decrease. It is clear from Figure 7 that the thermal temperature θ begins

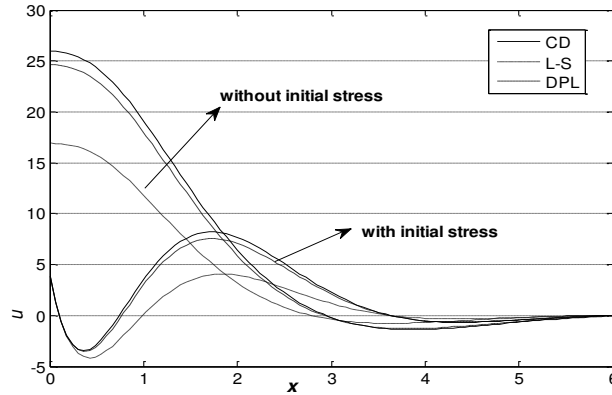


Figure 6. Horizontal displacement distribution u with initial stress and without initial stress.

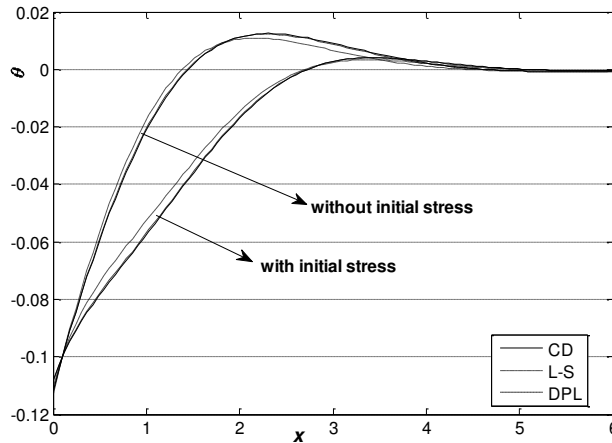


Figure 7. Thermal temperature distribution θ with initial stress and without initial stress.

from negative values and satisfies the boundary condition at $x = 0.1$. In the context of the three theories with without initial stress, θ increases in the range $0 \leq x \leq 6$. The values of θ decrease with initial stress. Figure 8 displays that the distribution of the stress component σ_{xx} begins from negative values and satisfies the boundary condition at $x = 0.1$. In the context of the three theories without initial stress, σ_{xx} starts with decreasing to a minimum value, and then increases. The initial stress, decrease, then increase, and last decrease values of σ_{xx} . Figure 9 shows the distribution of the stress component σ_{xy} , and demonstrates that it reaches a zero value and satisfies the boundary condition at $x = 0.1$. In the context of the three theories without initial stress, σ_{xy} starts with decreasing to a minimum value, and then increases. The initial stress increase and then decrease values of σ_{xy} . Figures 6–9 demonstrate that the initial stress has a significant role on all the physical quantities. Figures 10–12 show that the values of horizontal displacement components u , and the stress components σ_{xx} , σ_{xy} increase and then, decrease with reinforcement.

Due to the presence of reinforcement and initial stress, the magnitude of the thermophysical quantities

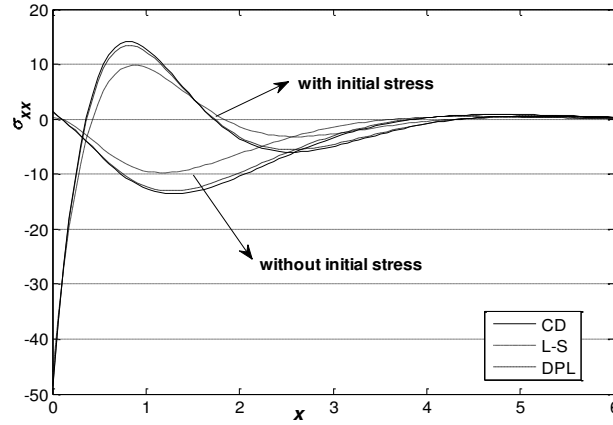


Figure 8. Distribution of stress component σ_{xx} with initial stress and without initial stress.

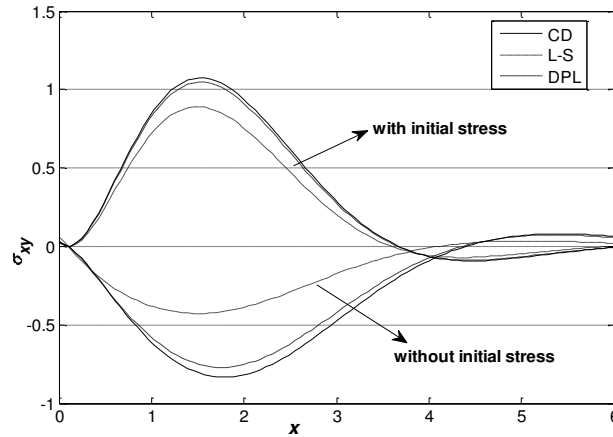


Figure 9. Distribution of stress component σ_{xy} with initial stress and without initial stress.

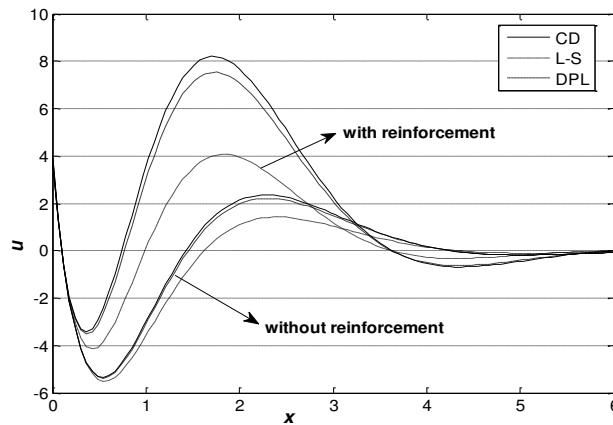


Figure 10. Horizontal displacement distribution u with and without reinforcement.

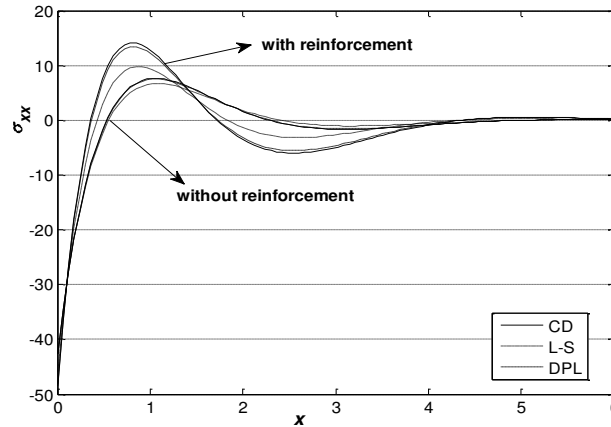


Figure 11. Distribution of stress component σ_{xx} with and without reinforcement.

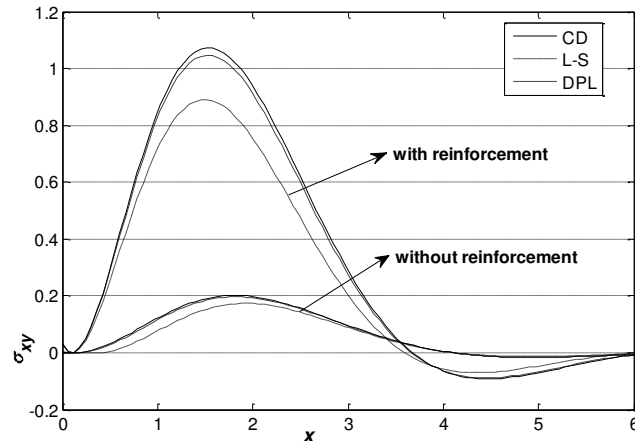


Figure 12. Distribution of stress component σ_{xy} with and without reinforcement.

decay, which indicates that initial stress and reinforcement have a tendency in maintaining the smoothness of the profiles of the thermophysical quantities. So it is more advantageous to consider the effect of initial stress and reinforcement in such problems of engineering.

In addition, for a fiber-reinforced generalized thermoelastic medium without temperature-dependent thermal conductivity ($K_1 = 0$) the results agree with the existing literature [Abbas and Abd-alla 2011].

8. Conclusion

In the present study, normal mode analysis is used to study the effect of the initial stress and temperature-dependent thermal conductivity on fiber-reinforced generalized thermoelastic medium based on the DPL theory, CD theory and the LS theory. We obtain the following conclusions based on the above analysis:

- (1) It is clear that the initial stress, temperature-dependent thermal conductivity, and the reinforcement play significant roles on all the physical quantities.

- (2) The phase lags τ_q and τ_θ has great influence on the distribution of all physical quantities.
- (3) The curves in the context of the DPL model, CD theory and the LS theory, decrease exponentially with increasing x ; this indicates that the thermoelastic waves are unattenuated and nondispersive, while purely thermoelastic waves undergo both attenuation and dispersion.
- (4) Deformation of a generalized thermoelastic medium depends on the nature of the applied force as well as the type of boundary conditions.
- (5) Analytical solutions based upon normal mode analysis of the thermoelastic problem in solids have been developed and utilized.

The results carried out in this paper can be used to design various fiber reinforced anisotropic media with initial stress in order to meet special engineering requirements.

References

- [Abbas and Abd-alla 2011] I. A. Abbas and A. N. Abd-alla, "Effect of initial stress on a fiber-reinforced anisotropic thermoelastic thick plate", *Int. J. Thermophys.* **32**:5 (2011), 1098–1110.
- [Abbas and Othman 2012] I. A. Abbas and M. I. A. Othman, "Generalized thermoelastic interaction in a fiber-reinforced anisotropic half-space under hydrostatic initial stress", *J. Vib. Control* **18**:2 (2012), 175–182.
- [Abbas et al. 2011] I. A. Abbas, A. N. Abd-alla, and M. I. A. Othman, "Generalized magneto-thermoelasticity in a fiber-reinforced anisotropic half-space", *Int. J. Thermophys.* **32**:5 (2011), 1071–1085.
- [Abdallah 2009] I. A. Abdallah, "Dual phase lag heat conduction and thermoelastic properties of a semi-infinite medium induced by ultrashort pulsed laser", *Prog. Phys.* **3** (2009), 60–63.
- [Abouelregal 2011] A. E. Abouelregal, "Generalized thermoelasticity for an isotropic solid sphere in dual-phase-lag of heat transfer with surface heat flux", *Int. J. Comput. Methods Eng. Sci. Mech.* **12**:2 (2011), 96–105.
- [Ailawalia and Budhiraja 2011] P. Ailawalia and S. Budhiraja, "Fibre-reinforced generalized thermoelastic medium under hydrostatic initial stress", *Engineering* **3**:6 (2011), 622–631.
- [Ailawalia et al. 2009] P. Ailawalia, S. Kumar, and G. Khurana, "Deformation in a generalized thermoelastic medium with hydrostatic initial stress subjected to different sources", *Mech. Mech. Eng.* **13**:1 (2009), 5–24.
- [Belfield et al. 1983] A. J. Belfield, T. G. Rogers, and A. J. M. Spencer, "Stress in elastic plates reinforced by fibres lying in concentric circles", *J. Mech. Phys. Solids* **31**:1 (1983), 25–54.
- [Biot 1956] M. A. Biot, "Thermoelasticity and irreversible thermodynamics", *J. Appl. Phys.* **27**:3 (1956), 240–253.
- [Biot 1965] M. A. Biot, *Mechanics of incremental deformations*, Wiley, New York, 1965.
- [Chandrasekharaiah 1986] D. S. Chandrasekharaiah, "Thermoelasticity with second sound: a review", *Appl. Mech. Rev. (ASME)* **39**:3 (1986), 355–376.
- [Cheng et al. 2000] J. C. Cheng, T. H. Wang, and S. Y. Zhang, "Normal mode expansion method for laser-generated ultrasonic Lamb waves in orthotropic thin plates", *Appl. Phys. B* **70**:1 (2000), 57–63.
- [Green and Lindsay 1972] A. E. Green and K. A. Lindsay, "Thermoelasticity", *J. Elasticity* **2**:1 (1972), 1–7.
- [Green and Naghdi 1993] A. E. Green and P. M. Naghdi, "Thermoelasticity without energy dissipation", *J. Elasticity* **31**:3 (1993), 189–208.
- [Hashin and Rosen 1964] Z. Hashin and B. W. Rosen, "The elastic moduli of fiber-reinforced materials", *J. Appl. Mech. (ASME)* **31**:2 (1964), 223–232.
- [Ignaczak and Ostoja-Starzewski 2010] J. Ignaczak and M. Ostoja-Starzewski, *Thermoelasticity with finite wave speeds*, Oxford University Press, New York, 2010.
- [Lord and Shulman 1967] H. W. Lord and Y. Shulman, "A generalized dynamical theory of thermoelasticity", *J. Mech. Phys. Solids* **15**:5 (1967), 299–309.

- [Montanaro 1999] A. Montanaro, “On singular surfaces in isotropic linear thermoelasticity with initial stress”, *J. Acoust. Soc. Am.* **106**:3 (1999), 1586–1588.
- [Nowacki 1975] W. Nowacki, *Dynamic problems of thermoelasticity*, Noordhoff, Leyden, The Netherlands, 1975.
- [Nowacki 1986] W. Nowacki, *Thermoelasticity*, 2nd ed., Pergamon Press, Oxford, 1986.
- [Othman and Abbas 2011] M. I. A. Othman and I. A. Abbas, “Effect of rotation on plane waves at the free surface of a fibre-reinforced thermoelastic half-space using the finite element method”, *Meccanica (Milano)* **46**:2 (2011), 413–421.
- [Othman and Said 2012] M. I. A. Othman and S. M. Said, “The effect of rotation on two-dimensional problem of a fibre-reinforced thermoelastic with one relaxation time”, *Int. J. Thermophys.* **33**:1 (2012), 160–171.
- [Othman et al. 2013] M. I. Othman, S. M. Said, and N. Sarker, “Effect of hydrostatic initial stress on a fiber-reinforced thermoelastic medium with fractional derivative heat transfer”, *Multidisc. Modeling Mater. Struct.* **9**:3 (2013), 410–426.
- [Quintanilla and Jordan 2009] R. Quintanilla and P. M. Jordan, “A note on the two temperature theory with dual-phase-lag delay: some exact solutions”, *Mech. Res. Commun.* **36**:7 (2009), 796–803.
- [Said and Othman 2016] S. M. Said and M. I. A. Othman, “Effects of gravitational and hydrostatic initial stress on a two-temperature fiber-reinforced thermoelastic medium for three-phase-lag”, *J. Solid Mech.* **8**:4 (2016), 806–822.
- [Said and Othman 2017] S. M. Said and M. I. A. Othman, “Effect of mechanical force, rotation and moving internal heat source on a two-temperature fiber-reinforced thermoelastic medium with two theories”, *Mech. Time-Depend. Mater.* **21**:2 (2017), 245–261.
- [Sarkar et al. 2016] N. Sarkar, S. Y. Atwa, and M. I. A. Othman, “The effect of hydrostatic initial stress on the plane waves in a fiber-reinforced magneto-thermoelastic medium with fractional derivative heat transfer”, *Int. Appl. Mech.* **52**:2 (2016), 203–216.
- [Sengupta and Nath 2001] P. R. Sengupta and S. Nath, “Surface waves in fibre-reinforced anisotropic elastic media”, *Sadhana* **26**:4 (2001), 363–370.
- [Tzou 1995a] D. Y. Tzou, “A unified field approach for heat conduction from macro- to micro-scales”, *J. Heat Transf. (ASME)* **117**:1 (1995), 8–16.
- [Tzou 1995b] D. Y. Tzou, “Experimental support for the lagging behavior in heat propagation”, *J. Thermophys. Heat Transf.* **9**:4 (1995), 686–693.
- [Tzou 1996] D. Y. Tzou, *Macro- to microscale heat transfer: the lagging behavior*, Taylor & Francis, Washington, DC, 1996.
- [Verma and Rana 1983] P. D. S. Verma and O. H. Rana, “Rotation of a circular cylindrical tube reinforced by fibres lying along helices”, *Mech. Mater.* **2**:4 (1983), 353–359.

Received 18 Apr 2018. Revised 23 Mar 2019. Accepted 2 May 2019.

MOHAMED I. A. OTHMAN: m_i_a_othman@yahoo.com
 Department of Mathematics, Faculty of Science, Zagazig University, Egypt

AHMED E. ABOUELREGAL: ahabogal@gmail.com
 Department of Mathematics, Faculty of Science, Mansoura University, Mansoura, Egypt

and

Department of Mathematics, College of Science and Arts, Aljuf University, El-Qurayat, Saudi Arabia

SAMIA M. SAID: samia_said59@yahoo.com
 Department of Mathematics, Faculty of Science, Zagazig University, Zagazig, Egypt

and

Department of Mathematics, Faculty of Science and Arts, Qassim University, Al-mithnab, Saudi Arabia

JOURNAL OF MECHANICS OF MATERIALS AND STRUCTURES

msp.org/jomms

Founded by Charles R. Steele and Marie-Louise Steele

EDITORIAL BOARD

| | |
|-----------------------|--|
| ADAIR R. AGUIAR | University of São Paulo at São Carlos, Brazil |
| KATIA BERTOLDI | Harvard University, USA |
| DAVIDE BIGONI | University of Trento, Italy |
| MAENGHYO CHO | Seoul National University, Korea |
| HUILING DUAN | Beijing University |
| YIBIN FU | Keele University, UK |
| IWONA JASLUK | University of Illinois at Urbana-Champaign, USA |
| DENNIS KOCHMANN | ETH Zurich |
| MITSUTOSHI KURODA | Yamagata University, Japan |
| CHEE W. LIM | City University of Hong Kong |
| ZISHUN LIU | Xi'an Jiaotong University, China |
| THOMAS J. PENCE | Michigan State University, USA |
| GIANNI ROYER-CARFAGNI | Università degli studi di Parma, Italy |
| DAVID STEIGMANN | University of California at Berkeley, USA |
| PAUL STEINMANN | Friedrich-Alexander-Universität Erlangen-Nürnberg, Germany |
| KENJIRO TERADA | Tohoku University, Japan |

ADVISORY BOARD

| | |
|---------------|---|
| J. P. CARTER | University of Sydney, Australia |
| D. H. HODGES | Georgia Institute of Technology, USA |
| J. HUTCHINSON | Harvard University, USA |
| D. PAMPLONA | Universidade Católica do Rio de Janeiro, Brazil |
| M. B. RUBIN | Technion, Haifa, Israel |

PRODUCTION production@msp.org

SILVIO LEVY Scientific Editor

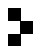
Cover photo: Mando Gomez, www.mandolux.com

See msp.org/jomms for submission guidelines.

JoMMS (ISSN 1559-3959) at Mathematical Sciences Publishers, 798 Evans Hall #6840, c/o University of California, Berkeley, CA 94720-3840, is published in 10 issues a year. The subscription price for 2019 is US \$635/year for the electronic version, and \$795/year (+\$60, if shipping outside the US) for print and electronic. Subscriptions, requests for back issues, and changes of address should be sent to MSP.

JoMMS peer-review and production is managed by EditFLOW® from Mathematical Sciences Publishers.

PUBLISHED BY

 **mathematical sciences publishers**
nonprofit scientific publishing

<http://msp.org/>

© 2019 Mathematical Sciences Publishers

Journal of Mechanics of Materials and Structures

Volume 14, No. 2

March 2019

- A mode-dependent energy-based damage model for peridynamics and its implementation**
CHRISTIAN WILLBERG, LASSE WIEDEMANN and MARTIN RÄDEL 193
- Elastic wave propagation in a periodic composite plate structure: band gaps incorporating microstructure, surface energy and foundation effects**
GONGYE ZHANG and XIN-LIN GAO 219
- Dynamic analysis of a mass traveling on a simply supported nonhomogeneous beam composed of transversely embedded periodic arrays**
YI-MING WANG and HUNG-CHIEH LIU 237
- Stress concentration around an arbitrarily-shaped hole in nonlinear fully coupled thermoelectric materials**
CHUAN-BIN YU, HAI-BING YANG, KUN SONG and CUN-FA GAO 259
- The effect of variable thermal conductivity on an infinite fiber-reinforced thick plate under initial stress**
MOHAMED I. A. OTHMAN, AHMED E. ABOUELREGAL and SAMIA M. SAID 277
- Large deflections and stability of spring-hinged cantilever beam** MILAN BATISTA 295



1559-3959(2019)14:2;1-W